Development of a 4-DoF Active Upper Limb Orthosis

robotics

MDPI

Article

Development of a 4-DoF Active Upper Limb Orthosis

Francesco Durante [1,*], Terenziano Raparelli [2] and Pierluigi Beomonte Zobel [1]

[1] Department of Industrial and Information Engineering and Economy (DIIIE), University of L'Aquila, P.le Pontieri 1, Località Monteluco, 67100 L'Aquila, Italy
[2] Department of Mechanical and Aerospace Engineering (DIMEAS), Politecnico di Torino, Corso Duca degli Abruzzi 24, 10129 Torino, Italy
* Correspondence: francesco.durante@univaq.it

Abstract: In this paper, the designs and manufacturing process of a powered upper limb orthosis are presented. The orthosis is an exoskeleton worn on one arm by the user and fixed to the trunk. The orthosis' architecture, design, and manufacturing process are presented and discussed. Estimations of the ranges of movement related to daily living activities are presented. The preliminary tests to verify the functionality of the design show encouraging results.

Keywords: active upper limb orthosis; kinematic analysis; dynamic analysis; pneumatic muscle; multibody model

Citation: Durante, F.; Raparelli, T.; Zobel, P.B. Development of a 4-DoF Active Upper Limb Orthosis. *Robotics* **2022**, *11*, 122. https://doi.org/10.3390/robotics11060122

Academic Editor: Girijesh Prasad

Received: 21 September 2022
Accepted: 30 October 2022
Published: 9 November 2022

1. Introduction

The continuous extension of the average life around the world means there will be more elderly people in the future. This is why the need for more and more sanitary care is expected, along with growing health costs. This is the main reason for the push to develop automated systems to apply medical therapies and assistance.

On the other hand, robots are increasingly present in daily life, from robots used for house cleaning to robots used for garden care. While the number of applications in which robots are useful in normal daily life continues to grow, the need for integration in the home environment and the need for safety in human–machine interactions are also growing. In this context, in recent years, collaborative robots and soft robotics, which meet these needs in biomedical, industrial, exploration, and human assistance fields [1–8], have received a lot of attention.

Such machines with high safety requirements certainly include robots used for motor rehabilitation and assistance.

There are two broad categories of active assistive machines based on how they mechanically interface with humans. The first category concerns machines of the end effector type, which work by being in contact only with the extremity of the limb being treated [9–17]. The second type relates to machines or devices of the exoskeletal type with a mechanical structure that reflects the skeletal structure of the limb, i.e., each segment of the limb associated with a joint movement is connected to the corresponding segment of the device [18–27].

Bio-inspired machines are more acceptable from a psychological point of view. The exoskeleton-type systems are bio-inspired, while the end effector ones are often the result of the adaptation of industrial robots. For safety purposes, these robots must be structurally compliant, and this often is achieved through the introduction of specific compliant devices. Compliance can also be achieved through control, but this is not always easy, such as when the transmissions are not back-drivable.

The exoskeleton-type machines also allow the user to control the individual joints, segment-by-segment, and to precisely guide the limb in complex movements. The end-effector-type machines are easier to use but can present critical issues related to the achievement of the singularity configurations of the human limbs.

The present work concerns an active orthosis for the upper limbs. The use of robots for support of the upper limbs has been studied and they have been used for some time. As for the actuators, they play a fundamental role in the device's safety. The most common robots used for upper limb aid are equipped with electric actuators [28–40]; however, pneumatic actuators [41–46], hydraulic actuators [47–50], actuators based on magnetorheological materials [51,52] or electrorheological materials [53], and actuators based on passive elastic elements combined with electric motors and functional electrical stimulation (FES) [54] or FES alone [55] are also used.

Although they are much less used for rehabilitation and assistive devices in general, and for devices dedicated to the upper limbs particularly, pneumatic muscle actuators are very interesting given their suitable characteristics for these devices [56–63]. They have a great power-to-weight ratio and are light, allowing them to be developed into easily transportable and wearable devices. They are inexpensive, flexible, and easy to place in the context of the machine, while not requiring precision in assembly. Finally, and very importantly, they are compliant. This feature confers compliance to the whole machine, making it intrinsically safe. Despite their advantages, they have the disadvantage of being more difficult to control than other actuators, since they are highly non-linear; sizing is difficult for the same reason. Several procedures and models are currently available for sizing pneumatic muscles [64–68]. Furthermore, they only work in one way and must be organized using an agonist–antagonist architecture. Their similarity to humans in appearance and operation brings another advantage; they are more acceptable and better suited to domestic contexts. Furthermore, their compliance, together with the antagonist–agonist configuration, allows for the variable stiffness of the joints [69].

Robots used for upper limb aids have distinct characteristics, especially for the exercise possibilities they allow. There are no standards regarding their performance; the various devices are distinguished by the joints or movements they can handle. There are robots designed for the shoulder [70], elbow [71–73], forearm [74], wrist [75,76], and finger joints [77–79], as well as for numerous joint combinations such as the shoulder and elbow [80,81]; forearm and wrist [82,83]; wrist and fingers [84]; shoulder, elbow, and forearm [85]; elbow, forearm, and fingers [86]; and forearm, wrist, and fingers [87]; or for the whole limb [88].

Control is a key part of an assistive robot. Cases where the control introduces compliance must be considered. Classic control strategies such as PID control are often used and work well in passive patient protocols. Other control systems are based on the sliding mode, mechanical impedance control, fuzzy logic [89], or combined approaches. Control systems usually use EMG signals [90,91], signals from measurements of kinematic parameters [92], dynamic parameters, or combinations of these factors [93].

Based on the analyzed literature, we conducted activities concerning the development of a device used to assist the upper limbs about the shoulder and elbow with a exoskeleton-type kinematic architecture. The device has four motorized degrees of freedom (DoF), actuated by pneumatic muscles. After the design phase, the orthosis was built. Certain preliminary experimental tests concerning the movements of the single joints were carried out. The validity of the project was proven.

Through a comparison conducted with similar devices, the proposed decide presents an innovative kinematic architecture that implements a spherical joint for the shoulder, motorizing all the three degrees of freedom. In this way, it is possible to perform physiologically correct movements. The orthosis performs well in terms of transparency and allows the specifications to be achieved while maintaining a small size. The kinematic architecture's novelty is in the way it implements a spherical joint, as described below. The abduction and adduction movements of the shoulder are achieved by means of a hinge, with an axis perpendicular to the frontal plane and passing through the center of the glenohumeral joint, which constrains a circular guide with a diameter matched to the above axis and with the center on the glenohumeral joint. Furthermore, there is a carriage part that is constrained to move on the guide, as if it were constrained by a second hinge

with its axis perpendicular to the plane of the guide versus the center of the guide. For the geometry described here, the carriage part is constrained to move on a spherical surface centered on the glenohumeral joint. The carriage part is the seat of a third hinge with an axis always coinciding with the center of the sphere and of the glenohumeral joint. This method of implementing a real spherical joint is innovative, as it has never been proposed before by other authors. Other solutions for the shoulder joint have three hinges with mutually perpendicular axes placed in series. These solutions are not spherical joints and do not perform as well. In fact, if an abduction movement of 90° is applied with an internal horizontal rotation movement of 90°, the shoulder is blocked in the extension movement. This extreme example highlights the device's limit, which in general is not so extreme. In any case, in a more general configuration, this limits the freedom of movement, which does not occur with the proposed joint. Another solution about a real spherical joint is presented that does not have the limit described but has larger dimensions, which is a disadvantage in terms of acceptability, and not all of the degrees of freedom of the joint are motorized, which is a disadvantage in terms of functionality. The novelty of the device is the use of pneumatic muscle actuators that reduce the mass and the overall dimensions, creating a device that performs well from the point of view of acceptability and is intrinsically safe thanks to the compliance achieved by the actuators. In the Discussion and Conclusions, a complete and detailed comparison of the proposed solution with other similar robots is presented and discussed.

2. Materials and Methods

2.1. Mechanical Design of the Orthosis

2.1.1. Technical Specification, Functional Design

As previously explained, the orthosis is designed for use as an assistive device for the upper limbs. The technical specifications that were considered for the design of the device are:

- Simple and low-cost design;
- Able to give more power to the movement of the upper arm;
- Sufficient power to move the hand with no aid from the biological muscles;
- The working volume for the hand is as large as possible to fit with activities of daily living;
- A payload of 5 N;
- Easy to wear and comfortable;
- Attention is paid to user acceptability.

The fact that it must be wearable directs the concept towards an exoskeleton-type device. Among the exoskeletons, there are exoskeletons with a structure and exosuits or soft suits with actuators integrated into the fabric. This second type of device can operate when the actuators are of the cushion or pneumatic bellows type and are interposed between two parts that must be separated, such as between the abdomen and pelvis for back support. These actuators are bulky and do not lend themselves to the case in question. The main problem with the soft suites is that the actuators integrated in the fabric of the suit, not having effective structural support, are unable to correctly apply the forces on the segments of the human body in order to implement the desired movements. Some authors have tried with reinforcement slats, but due to not being connected to each other by mechanical joints, these involve relative movements that reduce the efficiency of the transfer from the actuators to the user's body, also causing discomfort. The possible solution appears to be an exoskeleton with links connected by mechanical joints in such a way as to guide the movements by the actuators in a safe and precise manner. The links have appropriate cuffs for the application of loads to the segments of the human limb, with possible arrangements for connection to the structure that allow adaptations in order to compensate for the inevitable misalignments that are generated during the movements between the segments of the orthosis and the homologs of the human limb. Here, we only consider the shoulder and elbow joints.

As for the shoulder, the device, leaving out the shoulder girdle DoFs, must provide at least three rotational DoFs of the glenohumeral joint, which is a spherical joint. From these needs derives the difficulty of making a device that must reproduce a spherical hinge, with the center geometrically coinciding with the one of the glenohumeral joints inside the user's body. Then, three hinges with mutually orthogonal axes are required.

From the analysis of existing orthoses for the upper limb together with the design requirements, the functional design produced a device consisting of a frame fixed to the trunk [94]; for the abduction and adduction movements, a hinge is provided with an anteroposterior axis passing through the center of the humerus and containing the diameter of a semicircular profile articulated through this axis, with the trunk, and with a geometric center coinciding with the center of the humerus. The circular profile, with the limb extended along the body, has its axis in a vertical direction and is coincident with the longitudinal axis of the humerus. The semicircular element constitutes a guide that is articulated with a carriage, which given the architecture described here, can perform a rotational movement around the center of the humerus, i.e., the rotation movement of the shoulder. The carriage is the place of the third hinge, with a radial axis with respect to the guide, which is used for coupling with a link that runs parallel to the arm, allowing the flexion and extension movements of the shoulder. At the other end of the link there is another hinge at the elbow level that articulates the link corresponding to the arm with another corresponding to the forearm for flexion and extension movements of the elbow.

As for the range of motion (ROM), an investigation was carried out to measure the different human movements necessary for activities of daily living (ADL). A system based on inertial measurement units able to detect the movements of the human limb segments was used. By means of three IMUs, one placed on the trunk and the other two respectively on the arm and on the forearm, it was possible to detect the required ROM. The recording system was the Wear Notch motor capture interface, whose precision is 1.4 degrees for the angles. The investigated ADL were working at a desk, reading a book, writing, working at a PC, washing the face, brushing the teeth, scratching the nose, and activities for eating and drinking. A subject simulated the abovementioned ADL and the movements of the single segments of the upper limbs were recorded. In Figure 1, the subject during the simulations and the digital twin for the kinematic optimization are shown. In the same figure, the representative angles of the shoulder and of the elbow are shown.

By considering the results shown in Figure 1, the ROMs for the joints were chosen. The dimensions of the links were chosen according to the Hybrid III crash test dummy (Figure 2). The dimensions, ROMs and forces at the tip of the orthosis were as follows:

- Arm length a_3: 260 mm;
- Forearm length a_4: 340 mm;
- Shoulder abduction–adduction: $10° < \theta_1 < 80°$
- Shoulder external–internal rotation: $240° < \theta_2 < 330°$
- Shoulder flexion–extension: $70° < \theta_3 < 150°$
- Elbow flexion–extension: $0° < \theta_4 < 130°$
- Force on the end effector, F, 5 N, directed and pointing as gravity force.

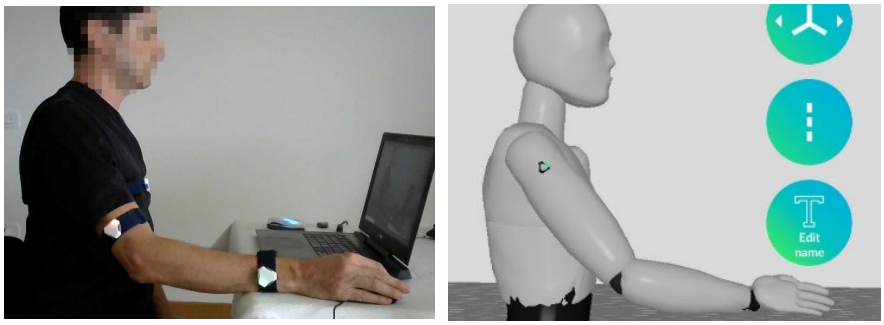

Figure 1. *Cont.*

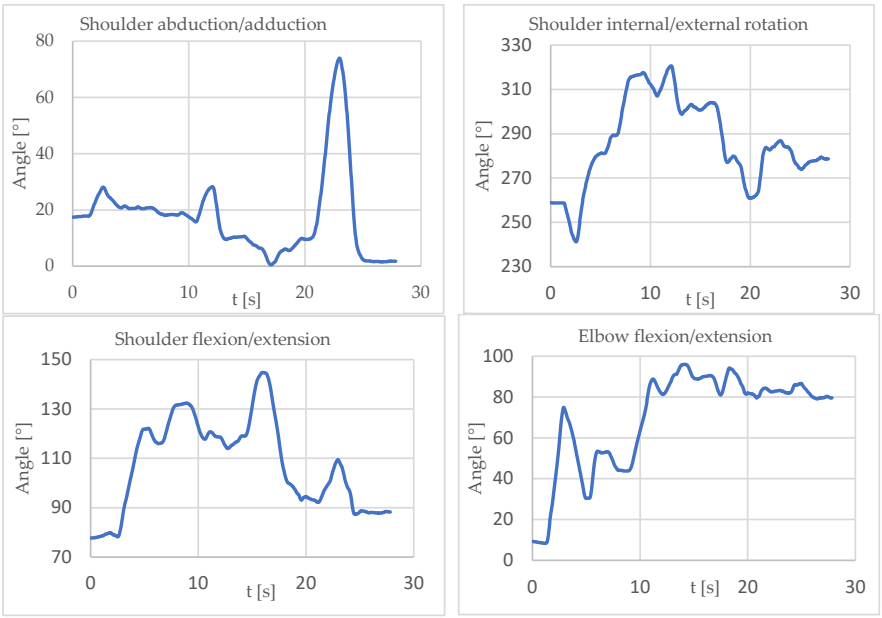

Figure 1. Simulations and recordings of upper limb movements in ADL (**above**). ROMs for the single joints in the chosen ADL (**bottom**). The references are the same as for the modified DH notation introduced for kinematic analyses and detailed in Figure 2.

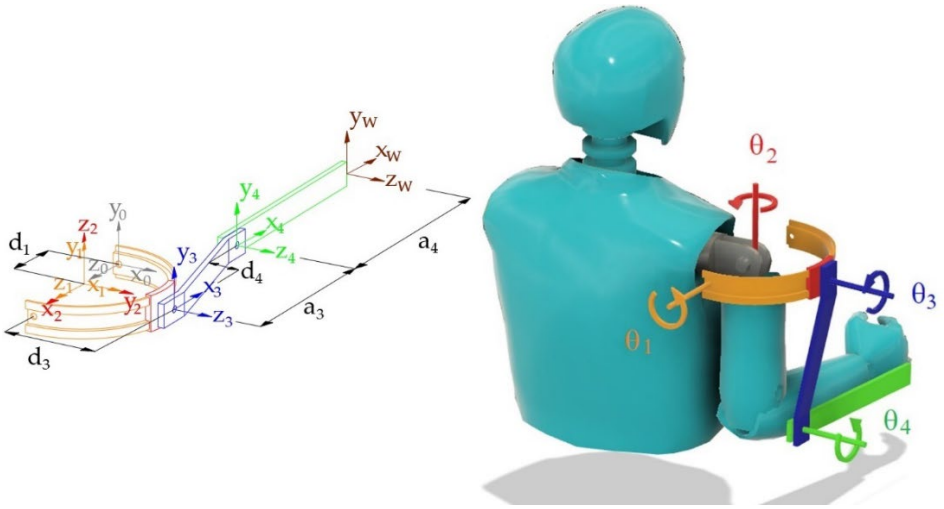

Figure 2. Kinematic architecture of the orthosis, geometrical dimensions, local references, and parameters for the kinematic analyses. On the left is the reference configuration θ^T = (0°, 270°, 180°, 0°) and on the right is the configuration θ^T = (0°, 270°, 90°, 90°).

2.1.2. Direct Kinematic Model Domain Analysis

For the determination of the working volume, the direct kinematic model was considered. Using the modified Denavit–Hartemberg notation, the transformation matrix between the reference frame of the wrist with respect to the base is given by the product of all single transformation matrices between link i and link i − 1:

$$ {}^{0}_{W}\mathbf{T} = {}^{0}_{1}\mathbf{T} \cdot {}^{1}_{2}\mathbf{T} \cdot {}^{2}_{3}\mathbf{T} \cdot {}^{3}_{4}\mathbf{T} \cdot {}^{4}_{W}\mathbf{T} \quad (1) $$

where in the considered case of the modified Denavit–Hartemberg notation [95]:

$$ {}^{i-1}_{i}\mathbf{T} = \begin{bmatrix} \cos\theta_i & -\sin\theta_i & 0 & a_{i-1} \\ \sin\theta_i \cos\alpha_{i-1} & \cos\theta_i \cos\alpha_{i-1} & -\sin\alpha_{i-1} & -\sin\alpha_{i-1} d_i \\ \sin\theta_i \sin\alpha_{i-1} & \cos\theta_i \sin\alpha_{i-1} & \cos\alpha_{i-1} & \cos\alpha_{i-1} d_i \\ 0 & 0 & 0 & 1 \end{bmatrix} \quad (2) $$

With reference to Figure 2, the numerical values of the parameters are shown in Table 1.

Table 1. Link parameters for the orthosis.

i	a_{i-1} [mm]	α_{i-1} [°]	d_i [mm]	θ_i [°]
1	0	0	100	θ_1
2	0	−90	0	θ_2
3	0	−90	100	θ_3
4	260	0	−42	θ_4
5 (W)	340	0	0	0

The orthosis ends with the wrist attachment point. The wrist is not present and a reference for the wrist, (W), was considered, which is rigidly connected with the extremity of the forearm.

From the matrix in (1), it is possible to determine the coordinates, with respect to the base, of any point, known as its coordinates with respect to the local reference of the wrist frame, for any set of joint angle values. By considering the position of the origin of the wrist frame in the local coordinates ($p = [0\ 0\ 0\ 1]^T$) and by varying the angles of the joints in the respective definition domains, the working volume of the device is determined. In Figure 3, the working volume is presented, with variations of 10° for θ_i, obtaining 10,080 different positions. The obtained point cloud was bounded and a triangular mesh surface was created in order to show the working volume.

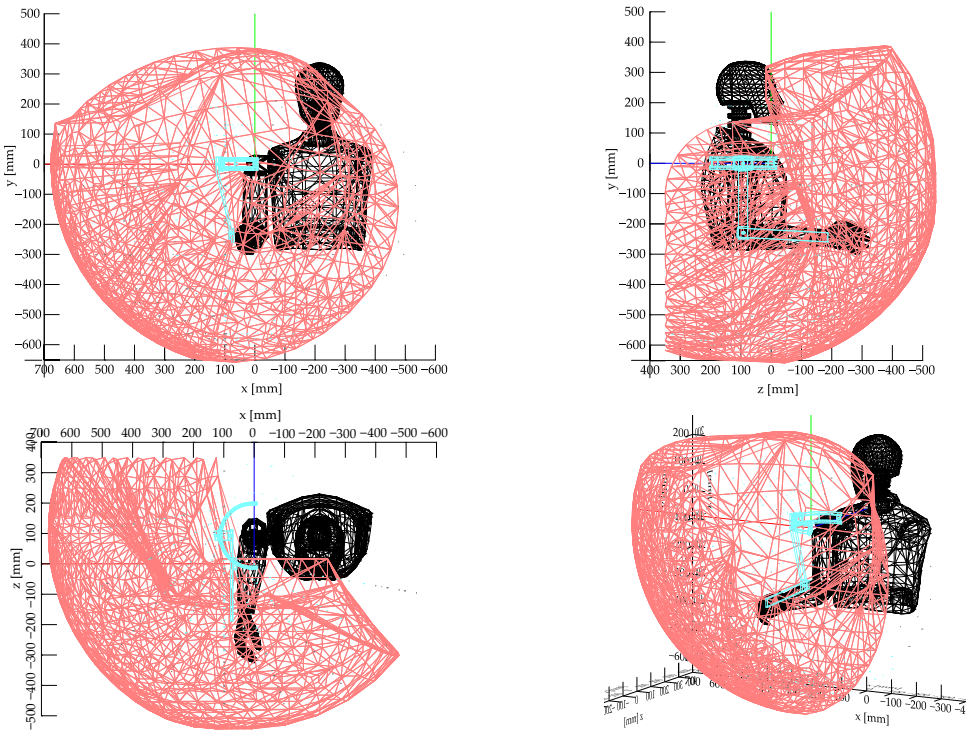

Figure 3. The working volume of the orthosis. The hand can comfortably reach the areas in front of the body, in front of the face, and up to the top of the head.

It can be seen that the volume of work is large in the areas in front of the trunk or face and in the lateral area above the head. It is understood that it is possible to operate on a table, bring objects to the mouth, and touch the face and the top of the head to take care of the person. In this case, the workspace investigation did not require a previous check of the congruence of the values of the joint parameters, which is required in the case of parallel kinematic chains [96]. As for the check of the risk of velocity fluctuations near singularity configurations, it can be stated that given the considered movements, the system will be quite far from those conditions and the relative consequences. In any case, the topic of kinematic velocity analyses through the Jacobian will be faced when the control system is implemented [97].

2.1.3. Dynamic Model

In order to determine the needed torque at the joints for the different movements, a dynamic model has to be considered. The equations of motion of the open kinematic chain have the following form:

$$H(q)\ddot{q} + h\left(q, \dot{q}\right) + C(q) = \tau \quad (3)$$

where q is the vector of the joint variables 4×1; $H(q)$ is the mass matrix, 4×4, which is symmetric and positively definite; $h\left(q, \dot{q}\right)$ is the vector of the centrifugal and Coriolis terms, 4×1; $C(q)$ is the vector of the gravitational terms, 4×1; τ is the vector of the torques applied to the joints, 4×1.

The equations were obtained using the Newton–Euler method [98]. By using local reference systems for each link, such as those provided by Denavit–Hartemberg's notation and already used for kinematic analyses, the equations of motion for the single link were written. In order to determine the inertial and Coriolis forces, the method provides a forward solution cycle, which starting from the base link, proceeds towards the end effector by solving the kinematics with given initial conditions and laws of motion. Then, we operate with a backward cycle, which starting from the end link proceeds towards the base with the writing of dynamic balances. At the end of the process, the torques exchanged at the i-th joint are obtained as a function of those applied to the i-th link and those exchanged with the next link (i + 1).

Each segment of the model consists of the structural element of the orthosis integrally connected to the homologous segment of the human body. The joints of the orthosis are considered to coincide with those of the human body.

The process was implemented in symbolic form (with Matlab Symbolic Toolbox software) and the matrix H and vectors h and C were obtained, from which the dynamic equations were obtained in closed form [98]. The usefulness of the method is that it can also operate with numerical data in real time; the calculation of the torque at the joints is more efficient than through equations in closed form and will be used in the future for the control of the device.

In this phase, in which there are no problems regarding the calculation time, the expressions of the couples at the joints were obtained and used in closed form. The matrices of Equation (3) are quite bulky so they are not reported.

Given that the device will have to operate at low speeds (max 30 mm/s), in the dynamic model, for the purpose of determining the numerical values of the torques at the joints, quasi-static laws of motion with zero speeds and accelerations were considered. in fact, kinetostatic conditions were considered. Table 2 shows the parameters that characterize the dynamic model.

Table 2. Parameters of the dynamic model.

Link i	m_i [kg]	d_{Gi} [m]	I_{xi} [kg m^2]	I_{yi} [kg m^2]	I_{zi} [kg m^2]
1	0.19	0.064	0.0009	0.0019	0.0009
2	0.01	0.100	0.0000	0.0001	0.0001
3	2.26 + 0.28	0.114	0.0028	0.0277	0.0277
4	1.35 + 0.26	0.118	0.0011	0.0105	0.0105
W	0.20	0.047	0.0002	0.0002	0.0002

An investigation was performed using this model of the parameters θ_i for I = 1, 4, and F, according to the values indicated above, and it was possible to determine the trends of the torque required at every joint as a function of the joint positions. Table 3 shows the maximum and minimum values of the required torques.

Table 3. Required torques at the joints of the orthosis.

	Maximum Torque [Nm]	Minimum Torque [Nm]
Shoulder abduction–adduction	22.05	4
Shoulder ext.–int. rotation	28.2	14.1
Shoulder flexion–extension	12	2.4
Elbow flexion–extension	7.5	−3.3

From these data, it is possible to trace the most critical movements for each joint in terms of the required torques, and to which the angles for which they occur can be associated. It is, therefore, possible to define the characteristics required by the machine for each joint.

2.1.4. Actuators, Transmissions

Regarding the actuation of the joints, pneumatic muscles were chosen in an agonist–antagonist arrangement. Among other advantages, the pneumatic muscle actuators ensure a high level of safety because of their compliance. A pulley-cable-type transmission was used for this purpose. As for the requirements of the actuators, the force, and the linear range, once the necessary torques for the joints were determined by the dynamic model, the diameter of the transmission pulleys must be chosen in order to determine the specifications of the pneumatic muscles. The pulleys must be chosen considering two conflicting needs. As the diameter increases, the forces required by the muscles decrease but their strokes increase. Therefore, the dimensioning of the muscles together with the transmission is a single process.

It was decided to use the McKibben pneumatic muscle actuators designed and manufactured by the authors [67].

The sizing of the actuators has been addressed by means of the results of a previous project relating to a lower limb orthosis. From that work, a pneumatic muscle with a diameter of 15 mm was found to be usable for the present project. As for the sizing of the actuators, let us consider the following. The force that can be developed by the pneumatic muscle depends on the diameter at rest and not on the nominal length (length at rest) for a given level of pressure, while the maximum shortening depends on the nominal length of the muscle. For the McKibben muscle, it is possible to have maximum shortenings close to 40%. Pneumatic muscles show characteristic force-shortening, which can be considered linear and typically has a trend ranging from the maximum force value, which occurs at zero shortening, to zero force, which occurs at maximum shortening. The characteristics of a muscle can, therefore, be determined by two points.

In the case in question, for the sizing of the pneumatic muscles, given that a muscle with a diameter of 15 mm is considered, this allows forces equal to 850 N at 0.7 MPa; with zero shortening, it is necessary to choose a maximum shortening of the muscle such that the

characteristics of the muscle are entirely above the characteristics required by the machine for the most critical movement. From the shortening, from the value of 40%, the length is obtained.

Two muscles positioned along the forearm drive the elbow joint, while the other two muscles positioned along the arm drive the shoulder flexion–extension. As for the shoulder's external–internal rotations, two muscles positioned in the back and connected to the carriage on the semicircular guide by a sheathed cable transmission drive the movements. Finally, two muscles, again positioned in the back, drive the abduction–adduction movements of the shoulder. These two muscles are not in an agonist–antagonist arrangement but work synergistically against the gravity driving the abduction, while the gravity provides for the opposite movement of adduction.

For the elbow joint, a radius for the pulley of 15 mm was chosen. For the flexion–extension of the shoulder, a radius of 20 mm was chosen for the pulley transmission. As for the external–internal rotations of the shoulder, the angular excursion from the design was 90°, which using a radius of the semicircular guide of 110 mm, gives an arc length of 170 mm. This would conduct to a pneumatic muscle with a rest length of about 425 mm, in which it is not possible to install the orthosis. Therefore, a transmission was considered with a ratio of i = 0.47, which is a movement multiplier. In this way, the pneumatic muscle rest length is reduced to about 200 mm. For the shoulder abduction–adduction transmission, a pulley with a radius of 30 mm was chosen.

Table 4 reports the functional characteristics of the muscles used in the 4 joints, while Figure 4 shows the traction force vs. contraction relations for the muscle used compared to the respective required characteristics of the joints. The working maximum operative pressure of the pneumatic muscles used is 0.7 MPa.

Table 4. Functional characteristics of the pneumatic muscles used in the orthosis.

	Length	Rest Diameter	Maximum Diameter	Maximum Force	Maximum Contraction
Shoulder flexion	190 mm	15 mm	27 mm	850 N	76 mm
Shoulder abduction	175 mm	15 mm	27 mm	2 × 850 N	70 mm
Shoulder rotation	220 mm	15 mm	27 mm	850 N	88 mm
Elbow flexion	175 mm	15 mm	27 mm	850 N	70 mm

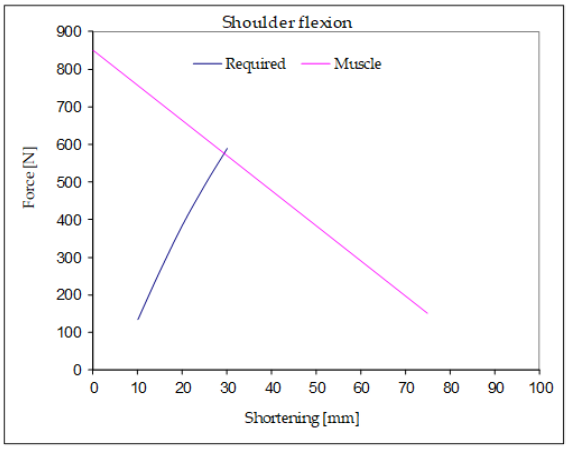

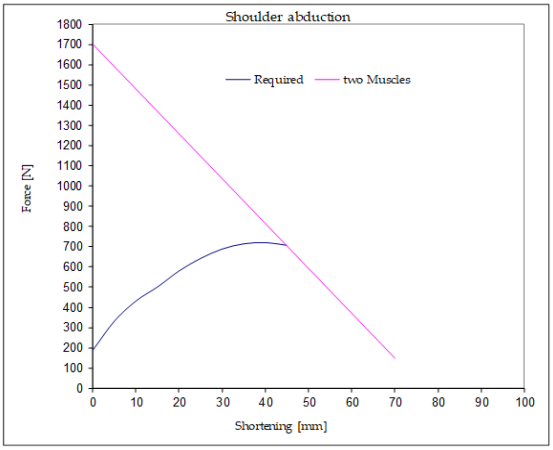

Figure 4. *Cont.*

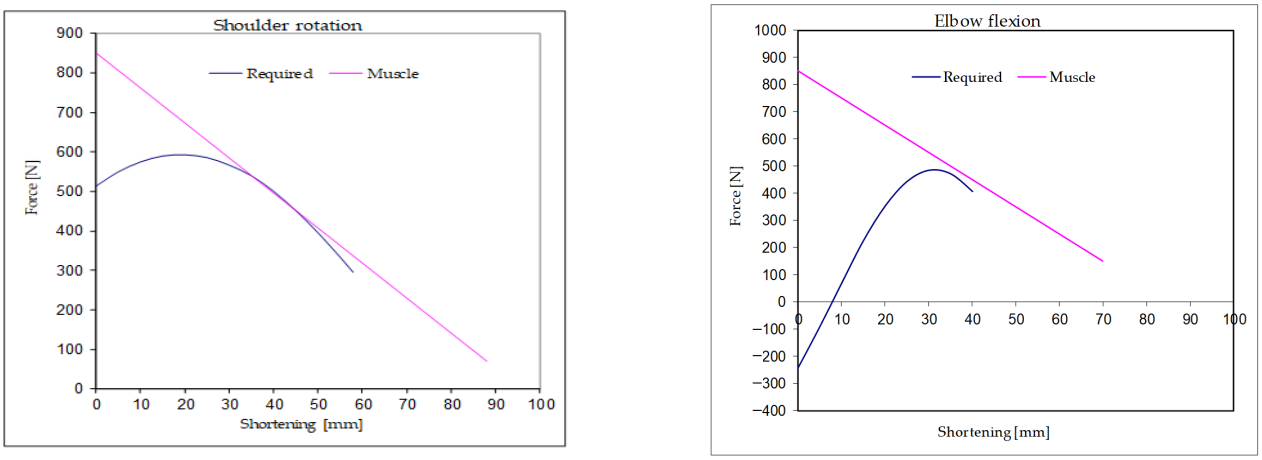

Figure 4. The sizing of the actuators is carried out by verifying that the required characteristic is always below the characteristic of the muscle for every joint.

2.1.5. Detailed Design

As for the detailed design for the purpose of optimizing the geometric dimensions, an approach based on verifications conducted with a multibody model (presented in the next paragraph) and on finite element models was followed. Proceeding through the repeated analyses, the definitive solution was reached with the aim of minimizing the overall dimensions, masses, and mechanical stresses.

So far we have talked about the mobile part of the orthosis, which is anchored to the user's chest. For anchoring, a frame is provided, which rests by means of two cuffs, one upper and one lower, on the trapezius and the iliac crest, respectively. The frame used for locking has two adjustable straps, one under the armpit and one on the side, which surround the trunk. In the anteroposterior direction on the frame, there are the seats for the hinge of the abduction and adduction movement of the shoulder allowed by the articulation of the semicircular guide with the frame (Figure 4). The frame is also the seat of the pneumatic muscles for the abduction and rotation movements of the shoulder (Figure 5).

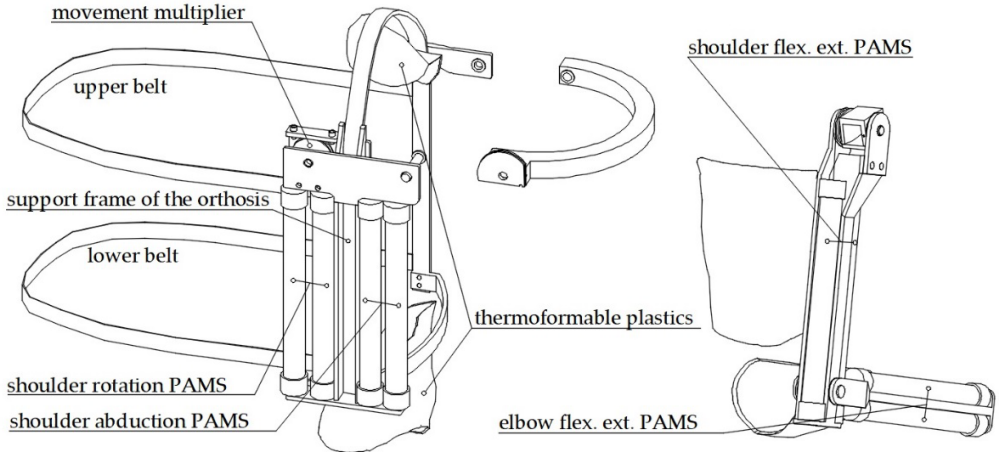

Figure 5. The frame for connection of the orthosis to the trunk and PAMS positioning.

The pulleys are connected to their respective links by screw couplings. The one that controls the abduction movement of the shoulder was made in one piece with the semicircular guide. For the rotation movement of the shoulder, the multiplication of the movement was obtained by means of a pair of integral pulleys with a ratio between the radii equal to 0.47.

The pneumatic muscles were made in house and steel ropes were considered for the transmission of movement. The mechanical interfaces were made using sheets of thermoformable plastic. All critical components have been verified, from a structural point of view, using FEM models (Figure 6). Figure 7 shows an overall view of the CAD project of the created orthosis.

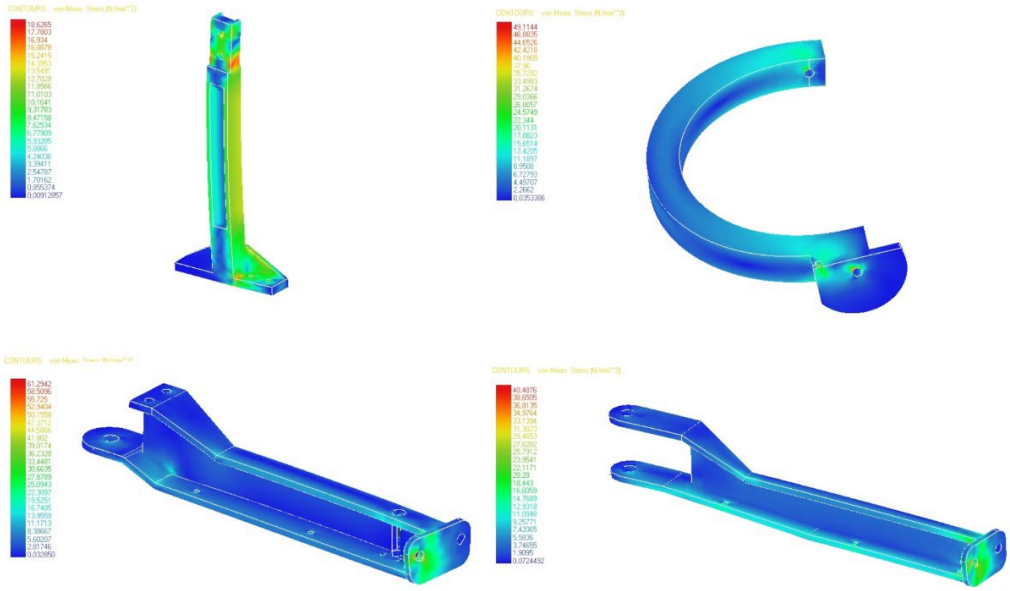

Figure 6. The structural sizing for the main components was carried out using finite element models.

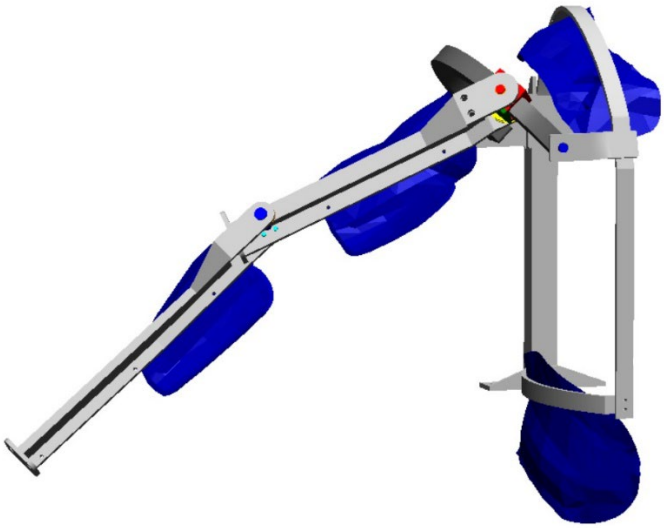

Figure 7. The 3D CAD modeling allowed the detailed dimensioning of all construction details.

2.1.6. Multibody Model

The design process, which is typically iterative, was characterized by checks on the dimensions, on the interference between the components, and on the actual performance in terms of the mobility using a three-dimensional multibody model. In particular, it was possible to verify the actual functionality in reaching three reference areas for daily life activities such as working on a table or desk, eating and drinking, and taking care of one's self.

The model of the mannequin was built on the basis of anthropometric data from Pheasant [99] and the online atlas Anatomy Learning [100], considering a male subject of average height in Italy, or 1.73 m, and the orthosis was based on the dimensions already

identified in the functional design phase. The joints of the mannequin were modeled with a spherical hinge for the shoulder and a flat hinge for the elbow. The joints of the orthosis are equipped with motors that make the device active. In this mode, movements in the joint space can be commanded and the model can be useful for evaluating the workspace and for solving inverse dynamics problems. The model was used, through repeated analyses, in order to obtain trajectories in space to verify the possibility of assisting in specific areas of the working volume. During the controlled movements, the congruence of the double kinematic chain (arm of the manikin and orthosis) was verified without interference between the various rigid members of the model, possibly making corrections in the CAD environment and reaching the final solution. The model was implemented using Simwise4D.

After verifying the basic movements of the individual DoF one at a time, the following movements were verified, to which one or more DoFs contribute:

1. Eating, drinking, taking care of yourself (wash your face, comb your hair, brush your teeth, etc.);
2. Grasping an object high above your head;
3. Touching your shoulder;
4. Touching your back;
5. Touching the nape of the neck;
6. Reaching the areas of a desk at which you are seated in order to carry out work activities such as reading, writing, and working on the computer.

Figure 8 shows a multibody model of the human together with the orthosis. It lacks the fastening straps to the trunk and the pneumatic muscles with the relative transmissions with sheathed ropes.

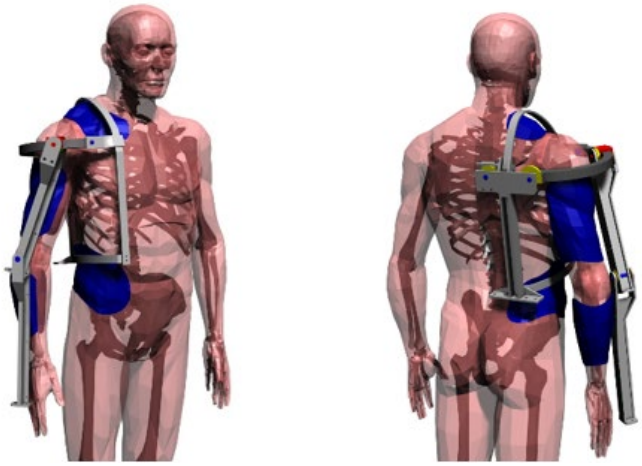

Figure 8. The complete multibody model with the mannequin and orthosis.

2.2. Control System

The control has to guarantee the stable and extremely robust dynamic functioning of the machine with respect to the uncertainties of the contacts in interactions with the user. It must modulate the response to mechanical perturbations and ensure a gentle and soft evolution both for safety reasons and good practice.

In the next paragraphs, we will discuss the hardware and strategy for the control, although they have not yet been implemented.

2.2.1. Hardware

Every joint is driven by a couple of muscles: the agonist and the antagonist. The supply and ventilation of the muscles are provided in two ways and in two positions via FESTO MHJ9 (FESTO, Esslingen am Neckar, Germany) high-frequency pulse width modulation (PWM)-driven digital valves. The digital valves will be driven by a microcontroller board.

The actual positions of the joints will be measured by a conductive plastic potentiometer. This is a precision potentiometer with an electric arc of 340 degrees, 10 kΩ of electric resistance, and 2% linearity accuracy.

As for the energy autonomy, this will be provided by means of an electric battery, a small air compressor, and a very small tank to smooth the pressure fluctuations. There is a need for 14 valves. The FESTO MHJ9 value measures 9 mm × 32 mm × 51 mm, so it will be placed in a box measuring 126 mm × 51 mm × 32 mm. All components will be placed in a backpack, while in domestic environments the devices can work with a ground compressor and an air distribution pipe. In this way, the compressor will not be on board and the device will be lighter.

As for the other sensors (for the interface with the user), they depend on the control strategy and will be discussed in the next paragraph.

2.2.2. Control Strategy

The control of exoskeletal devices can be based on two approaches, one with trajectory control in which the machine does everything once it has the command, and the one with interaction control, in which the machine, during movement, continuously exchanges information with the user. Trajectory control is forced when the user's limb is unable to generate signals because muscle contractions are absent. In this case, it is possible to proceed with pre-established trajectories that can be controlled with eye tracking systems or with voice command systems. The control of the trajectories can be implemented using fuzzy control, as implemented by the authors for a rehabilitation arm [101]. Fuzzy logic control (FLC) is particularly suitable considering the characteristics of the pneumatic muscles for compliance and non-linear behavior. The most notable feature of an FLC is the "translation" of fuzzy linguistic rules and measurements into non-linear mapping. An FLC can be adjusted through practical observations or experience, almost ignoring the complexity of the system, and can deal with complex systems with relative ease, while still providing robustness and logical interpretability because it can handle uncertainty (system variations, sensor noise), being defined in an uncertain way [101].

In the event that the user's limb is able to generate signals, it is advisable to use these for control, both because the user can operate it in a more natural way and because the commitment to controlling the limb can have a rehabilitative function. In this case, the user will be the central element of the control and command process, and through sight and the proprioceptive system will verify the movement to make corrections according to their intentions. The machine will be equipped with sensors to detect the intention and will be able to apply forces on the environment, the references of which are generated by the user. Based on the observation of the evolution of movements, the user will correct the force references by comparing them with the relative references (also generated by the user). Overall, the human–machine system will control the mechanical impedance of the system itself.

For the application of the forces, it is possible to proceed with pressure sensors, for each pneumatic muscle, which allow, together with the knowledge of the current deformation, the force developed by the muscle to be traced and the torque to be applied to the joint.

As for the sensors for the user's intention, the simplest system is to use myoelectric sensors capable of detecting the activity of human muscles homologous to those of the orthosis. In this way, it is sufficient to control the actuators directly without having to carry out calculations through dynamic models to trace the torques to be applied at the level of the joints. This solution has the disadvantage of having to position the EMG sensors accurately in at least four points of the user's limb. In the same way, the airbag sensors already used by the authors in a lower limb orthosis can be used [20]. Another possibility is to use an interaction sensor between the human and the machine. A load cell with three axes placed at the end of the orthosis connected to the user's wrist can work. The detected force can be used by controlling the orthosis so that it is applied to the environment with the end effector, a force equal to that detected and increased according

to a desired amplification factor. In this case, it is necessary to use a dynamic model that in real time provides the required torque values to the joints. The model is the one described in Section 2.1.2.

3. Results

3.1. Multibody Model

The multibody model highlights that the movements for working on a bench, eating and drinking, and caring for the one's self can be performed, while there is a limitation in reaching positions behind the frontal plane due to the absence of the shoulder anteposition movement (Figures 9–12).

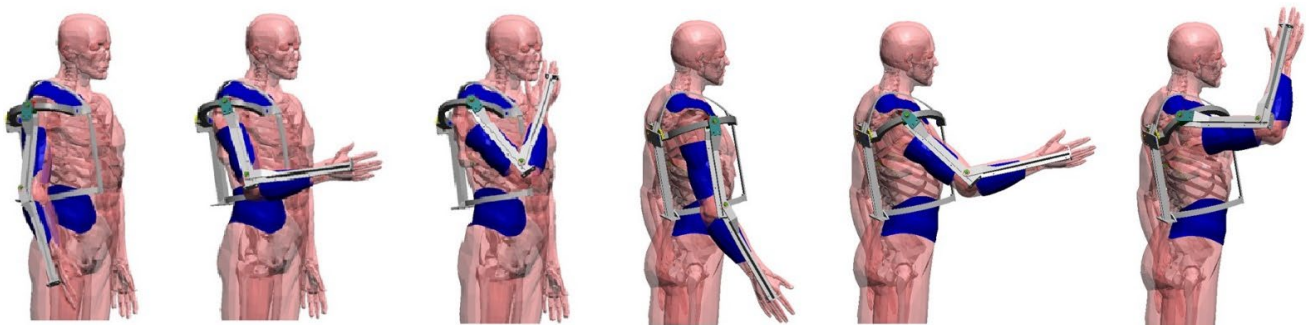

Figure 9. Simulations for reaching the face and the part above the head, for which the verification is positive.

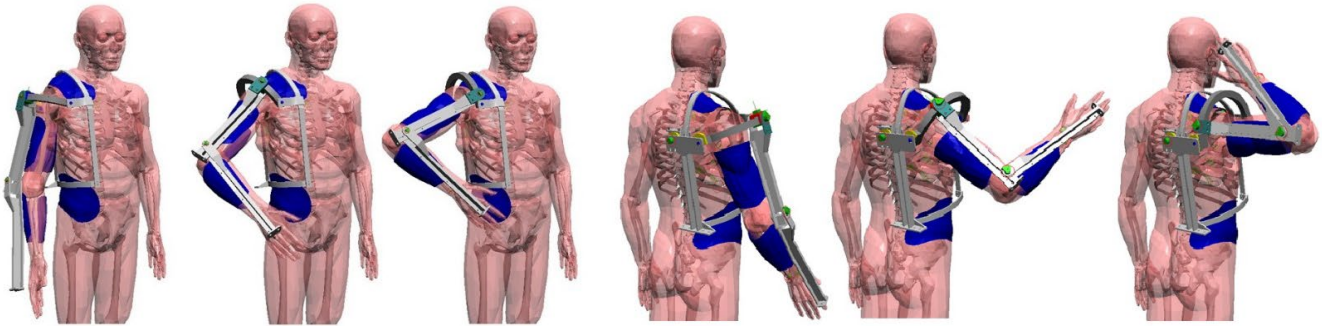

Figure 10. Simulations for reaching the areas behind the pelvis and behind the neck. In these movements the system fails.

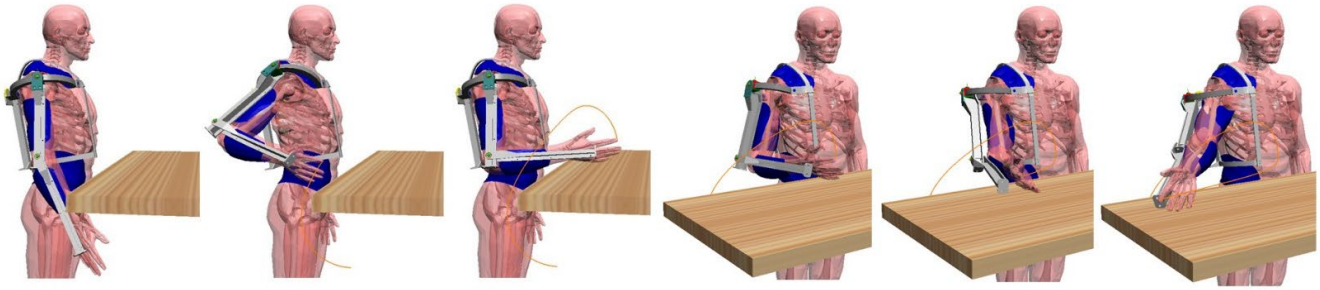

Figure 11. Simulations for reaching a desk top and the area on the right.

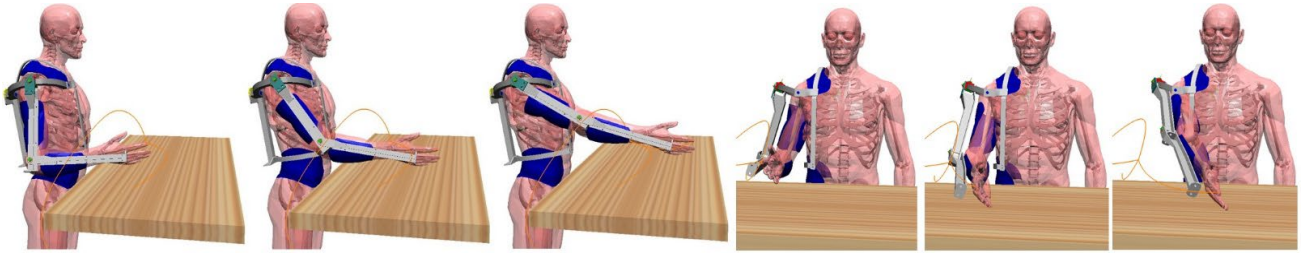

Figure 12. Simulations for reaching the front area of a desktop and the area on the left.

3.2. Orthosis Prototype

The orthosis was made using aluminum for the structural parts and steel for the hinge pins and the body of the trolley for shoulder rotation. The connection of the muscles to the transmission cables was made by means of small pieces of steel, in which the rope is engaged by a stop for motorcycle applications (Figure 13). The other end of the muscle is locked on the orthosis by means of a nut on a thread placed on the head of the muscle (Figure 13). Beyond the nut is a quick connection for the air tube for feeding and ventilation. The thermoformable plastics are made of nylon by customizing them to the subject for which special plaster casts were created and then used in forming the nylon sheets. The valves were connected to their parts through screws (Figure 13). The thermoformable plastics were equipped with Velcro strings for quick fastening on the user's body. In particular, the shoulder was covered on the side in contact with the human body with a layer of foam rubber for increased comfort (Figure 14).

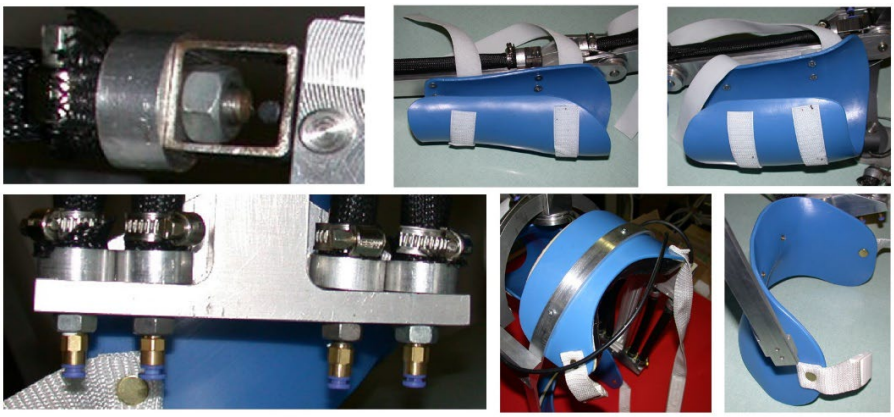

Figure 13. Construction details. Pneumatic muscles and mechanical and pneumatic connections. The cuffs for the arm, forearm, shoulder, and pelvis.

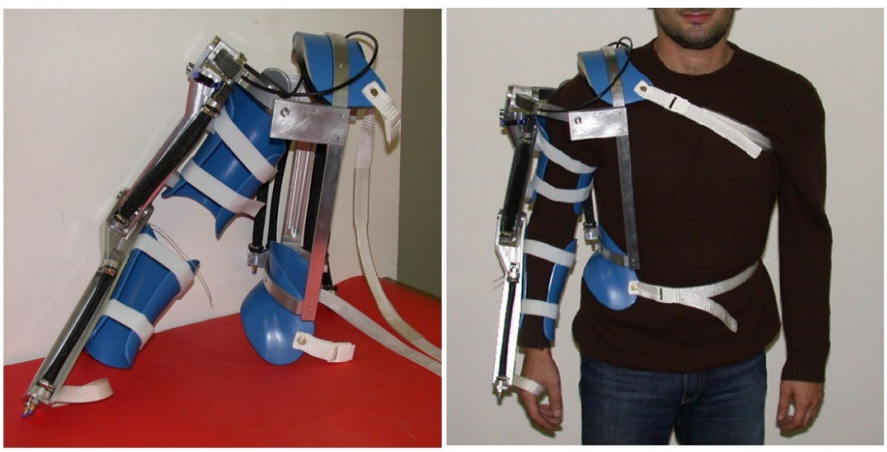

Figure 14. The device and a wear test.

3.3. First Experimental Tests

To carry out preliminary checks on the functionality of the orthosis, a manually controlled pneumatic circuit was created to feed the pneumatic muscles. It consisted of solenoid valves, switches, and flow regulators, as shown in Figure 15.

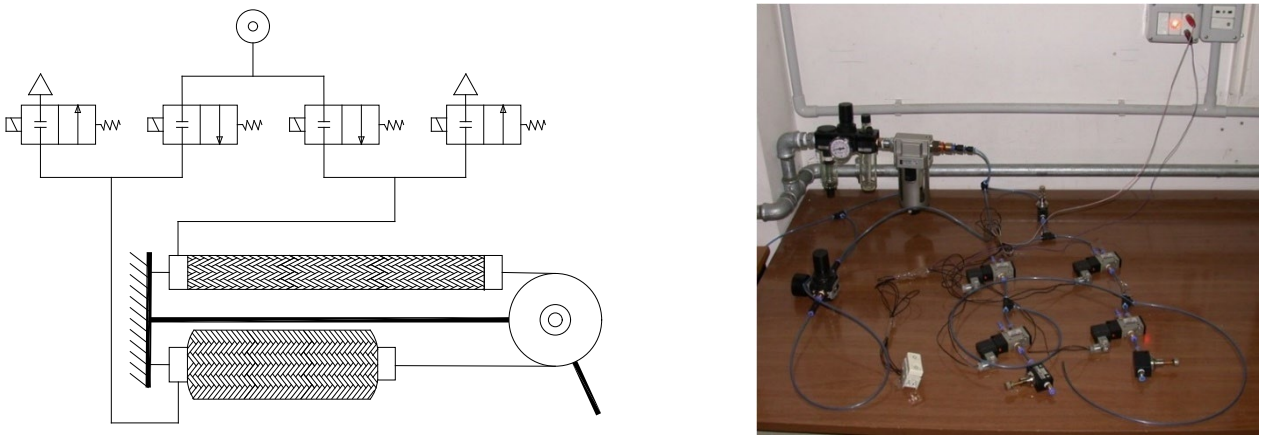

Figure 15. Diagram and experimental setup of the pneumatic circuit used for the first tests.

Using this circuit, it was possible to control the movements through the individual DoFs. The command through the circuit allows pressurized air to be sent up to the design pressure equal to 0.7 MPa. The tests consisted of controlling the movements with the passive user until the maximum working pressure was reached. In the starting configuration for each DoF, the limb was extended along the body for elbow flexion and shoulder flexion and abduction movements. For shoulder rotation, in the starting position the elbow was flexed at 90° with the shoulder in 90° abduction and with the maximum possible internal rotation (60°).

For the purpose of the initial quantitative assessments, rough video footage was taken with a camera with an optical axis perpendicular to the sagittal plane for flexion movements and to the frontal plane for the shoulder abduction movement.

Key frames were extracted from the videos, which allowed post-processing to the CAD for verification. Figures 16–18 show the post-processed frames.

Figure 16. Shoulder abduction range: 5–77°.

Figure 17. Shoulder flexion range: 70–127°.

Figure 18. Elbow flexion range: 10–107°.

Tests were conducted for each degree of freedom, one movement at a time. An operator other than the user controlled the entry of air into the affected pneumatic muscles by means of a manually operated pressure regulator. By means of a pressure gauge on the delivery pipe, it was possible to verify that the design pressure of 0.7 MPa was reached. During the tests, the air was delivered at time intervals of about 5 s, but given the rapid response of the actuators, the movements can be carried out more quickly. The tests gave repeatable results.

4. Discussion

As mentioned, the multibody model shows that with the orthosis it is possible to carry out activities of daily life, such as taking care of one's self, eating, drinking, working at a table, reading, writing, and working on a computer. However, it was difficult to bring the hand behind the back and to the nape of the neck. In particular, it can be seen that for the movement to bring the hand behind the back, in overcoming the frontal plane the carriage for the rotation of the shoulder reaches the end of its travel path on the circular guide during internal rotation. Similarly, to reach the position behind the nape, in an attempt to overcome the frontal plane, the trolley for the rotation of the shoulder reaches the end of its travel path on the circular guide during external rotation. This limit cannot be exceeded, since the guide cannot develop a useful angle greater than 180° and the carriage has a non-zero angular dimension (approximately 40°). If this limit is to be exceeded, the orthosis should also be able to implement the anteposition movements of the shoulder. However, these movements are of no great interest in normal daily life.

As far as the prototype is concerned, the first observation concerns the kinematic transparency and wearability. No difficulties were found in the context of the planned mobility and no difficulty was found in the case of use over clothes. Some problems were instead identified in the case of use under clothing. It is necessary to apply protections for the hinges to avoid damage to clothing, as well as the use of padding for plastics to prevent slipping and to make the orthosis comfortable. Another target of the project was lightness. The device, complete with the muscles, has a mass of 4.4 kg. A great help in supporting the orthosis by the user is provided by the pelvic grip, which allows the user to unload most of the weight onto the pelvis.

As for the first experimental tests, it was found that the movements performed for the flexion of the shoulder and the elbow are of a smaller amplitude than those planned, while the abduction of the shoulder meets the requirements. In particular, the movements range from 5° to 77° with an excursion of 72° against a design requirement equal to 70°. For the rotation of the shoulder, the movements are mainly not hindered by the action of gravity, which is generally orthogonal to the direction of the movements. As for the check, the internal rotation is favored in the chosen configuration. While the external rotation is performed in the most critical conditions, it is still possible to reach the position equal to −20° against a requirement angle of −30°due to the friction in the sliding of the carriage with respect to the guide.

For the shoulder extension–flexion, the movements range from 70° to 127° with an excursion of 57° against a design excursion of 80°. In particular, for maximum flexion, the position reached of 127° is 23° from the target position of 150°. For the flexion of the elbow, the movements range from 10° to 107°. Here, the data that matter are for the final position, which must be compared with the 130° design requirement, meaning there is a gap of 23°. These differences are partly due to the compliance of the devices for connecting the transmission ropes to the pneumatic muscles. During the tests, deformations of 1–2 mm were detected. With these deformations and a pulley radius equal to 15 mm, there was a loss in terms of angular excursion equal to about 10°. Another cause was evidently the lack of force developed by the pneumatic muscles due to the friction and resistance (human limb, clothes, etc.) not being correctly estimated. In fact, for the abduction movement, for which two muscles were used in parallel and coupled by means of a barbell, the requirement was reached.

In order to provide evidence of the advantages brought about by the proposed device, a comparison was carried out with similar devices found in the literature. The comparison was based on the degrees of freedom that the orthosis has for the shoulder and elbow joints, on whether they are motorized or not, on whether the shoulder has a spherical joint, on the amplitudes of the various movements, and on the acceptability of the device by the user. Figure 19 shows the considered orthoses and Table 5 shows a comparison of the proposed device with the others under study.

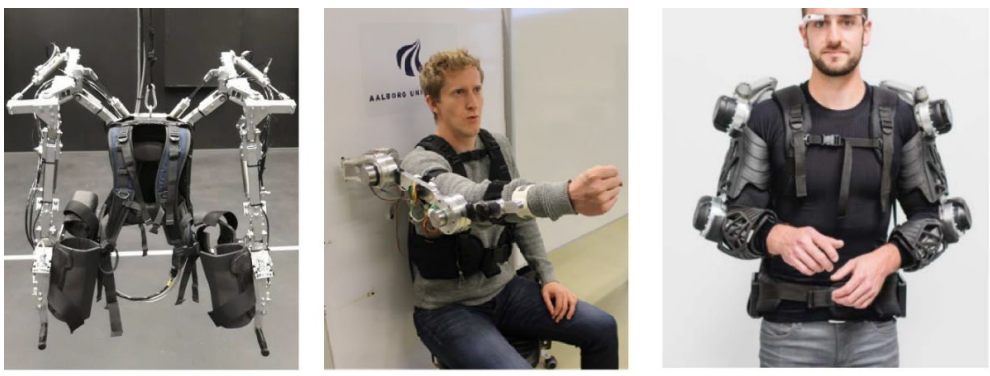

(a) (b) (c)

Figure 19. *Cont.*

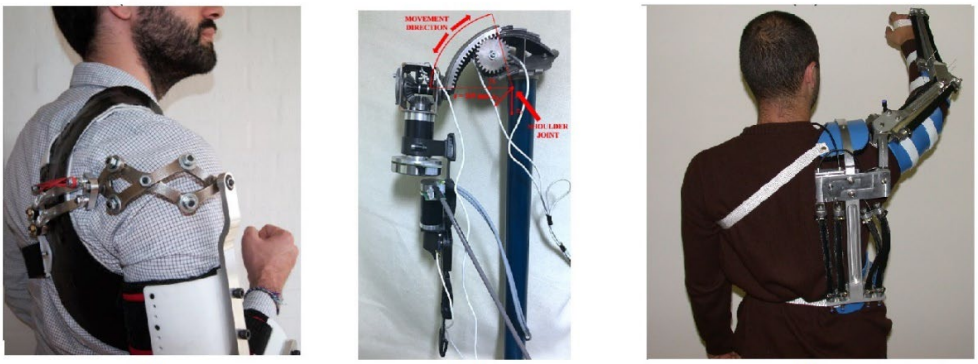

(**d**) (**e**) (**f**)

Figure 19. The five orthoses used for comparison with the proposed device: (**a**) Inferno upper limb exoskeleton. Reprinted with permission from ref. [102]. Copyright 2018 IEEE; (**b**) UB-AXO by Aalborg University. Reprinted with permission from ref. [103]. Copyright 2017 IEEE; (**c**) Stuttgart Exo-Jacket. Reprinted with permission from ref. [104]. Copyright 2017 IEEE; (**d**) compact 3 degrees-of-freedom scissor linkages for an upper limb exoskeleton. Reprinted with permission from ref. [105]. Copyright 2019 Elsevier; (**e**) link set sliding for an abduction-adduction upper limb exoskeleton. Reprinted from ref. [106]; (**f**) our proposed orthosis.

Table 5. Characteristics of the orthoses under comparison. SAA = shoulder abduction–adduction; SR = shoulder rotation; SFE = shoulder flexion–extension; EF = elbow flexion; S.Shp.J. = shoulder spherical joint; a = active; p = passive; na = data not available; np = not present. Brackets (**a**)–(**f**) correspond to the devices shown in Figure 19; (**g**) represents the reference requirements.

Device	SAA	SR	SFE	EF	S. Sph. J.	Acceptability
(**a**)	0°/45°, a	240°/270°, a	90°/210°, a	0°/90°, a	✗	✗
(**b**)	0°/90°, a	240°/380°, p	30°/260°, a	na, a	✔	✔
(**c**)	na, a	np	na, a	na, a	✗	✔
(**d**)	na, p	na, p	na, p	na, p	✔	✔✔✔
(**e**)	0°/60°, a	240°/380°, a	np	0°/130°, a	✗	✗
(**f**)	5°/77°, a	250°/320°, a	80°/127°, a	10°/107°, a	✔	✔✔
(**g**)	10°/80°, a	240°/330°, a	70°/150°, a	0°/130°, a	✔	✔✔✔

From the comparison results, as for the ROMs, some devices outperform the requirements, while the proposed one does not completely satisfy the requirements for EF and SFE. On the other hand, regarding the kinematic architecture, the proposed device is among the few implementing three DoFs for the shoulder joint. Moreover, the proposed solution is a spherical joint in a device, which at the same time is wearable.

Of the five devices compared here, one presents only two DoFs for the shoulder joint, while the remaining four present three DoFs. Two of them do not form a spherical joint (because the DoFs, although orthogonal, are placed in series), and this is a constraint that the spherical joint does not present. As for the other two, a spherical joint is implemented; one of them is without any actuation, while for the other the rotational movement is not motorized. As for the acceptability, the best device is not motorized; two are unacceptable due to being bulky. The two acceptable devices present a lack of DoFs or motorization. Therefore, the proposed device is the only one implementing a spherical joint for the shoulder with all DoFs being motorized, which is also reasonably small and acceptable. From the comparison, it can be concluded that the proposed device has a better score for the considered requirements.

5. Conclusions and Future Development

Overall, it can be said that the verifications have shown the validity of the project, since the differences from the requirements can be overcome.

In the future, more attention will be paid to the critical aspects highlighted here. In particular, more rigid systems for attaching the ends of the transmission cords will be considered to reduce errors due to compliance. Larger diameter pneumatic muscles will be used in order to provide greater strength for flexion–extension and rotation movements of the shoulder and for flexion–extension movements of the elbow in order to completely satisfy the requirements. Finally, the possibility of using a carriage equipped with rolling elements to couple the circular guide for the rotation movement of the shoulder will be considered. A weakness of the proposed device is the lack of adaptability to the different anthropometric dimensions of different user. This will be achieved by using a new design for the arm in two pieces with an adjustable connection. Once the functionality is achieved, the control system will be implemented and the system will be completely characterized.

Author Contributions: Conceptualization, F.D.; methodology, F.D., P.B.Z., and T.R.; validation, F.D.; formal analysis, F.D., P.B.Z., and T.R.; investigation, F.D., P.B.Z., and T.R.; data curation, F.D.; writing—original draft preparation, F.D.; writing—review and editing, F.D.; visualization, F.D., P.B.Z., and T.R.; supervision F.D., P.B.Z., and T.R. All authors have read and agreed to the published version of the manuscript.

Funding: This research received no external funding.

Informed Consent Statement: Informed consent was obtained from all subjects involved in the study.

Data Availability Statement: Not applicable.

Acknowledgments: The authors gratefully acknowledge the contribution of dott. Fabrizio Raparelli in the experimental test reported in this paper. All individuals included in this section have consented to the acknowledgment.

Conflicts of Interest: The authors declare no conflict of interest.

References

1. Majidi, C. Soft Robotics: A Perspective—Current Trends and Prospects for the Future. *Soft Robot.* **2014**, *1*, 5–11. [CrossRef]
2. Shiomi, M.; Nakagawa, K.; Shinozawa, K.; Matsumura, R.; Ishiguro, H.; Hagita, N. Does A Robot's Touch Encourage Human Effort? *Int. J. Soc. Robot.* **2017**, *9*, 5–15. [CrossRef]
3. Antonelli, M.G.; Zobel, P.B.; D'ambrogio, W.; Durante, F. Design methodology for a novel bending pneumatic soft actuator for kinematically mirroring the shape of objects. *Actuators* **2020**, *9*, 113. [CrossRef]
4. Banerjee, H.; Tse, Z.T.H.; Ren, H. Soft robotics with compliance and adaptation for biomedical applications and forthcoming challenges. *Int. J. Robot. Autom.* **2018**, *33*, 69–80. [CrossRef]
5. Shintake, J.; Cacucciolo, V.; Floreano, D.; Shea, H. Soft Robotic Grippers. *Adv. Mater.* **2018**, *30*, 1707035. [CrossRef]
6. Antonelli, M.G.; D'Ambrogio, W.; Durante, F. Development of a pneumatic soft actuator as a hand finger for a collaborative robot. In Proceedings of the ICMSCE International Conference, Amsterdam, The Netherlands, 22–23 February 2018; pp. 67–71. [CrossRef]
7. Yang, Y.; Chen, Y.; Li, Y.; Chen, M.Z.Q.; Wei, Y. Bioinspired robotic fingers based on pneumatic actuator and 3D printing of smart material. *Soft Robot.* **2017**, *4*, 147–162. [CrossRef]
8. Antonelli, M.G.; Zobel, P.B.; Durante, F.; Raparelli, T. Additive manufacturing applications on flexible actuators for active orthoses and medical devices. *J. Healthc. Eng.* **2019**, *2019*, 5659801. [CrossRef]
9. Ellis, M.D.; Sukal, T.; DeMott, T.; Dewald, J.P.A. ACT 3D Exercise targets gravity-induced discoordination and improves reaching work area in individuals with stroke. In Proceedings of the IEEE 10th International Conference on Rehabilitation Robotics ICORR. Noordwijk, The Netherlands, 13–15 June 2007; pp. 890–895.
10. Ju, M.S.; Lin, C.C.K.; Lin, D.H.; Hwang, I.S.; Chen, S.M. A rehabilitation robot with force-position hybrid fuzzy controller: Hybrid fuzzy control of rehabilitation robot. *Ieee Trans. Neural Syst. Rehabil. Eng.* **2005**, *13*, 349–358. [CrossRef]
11. Micera, S.; Carrozza, M.; Guglielmelli, E.; Cappiello, G.; Zaccone, F.; Freschi, C.; Colombo, R.; Mazzone, A.; Delconte, C.; Pisano, F.; et al. A simple robotic system for neurorehabilitation. *Auton. Robot.* **2005**, *19*, 271–284. [CrossRef]
12. Sulzer, J.S.; Peshkin, M.A.; Patton, J.L. Design of a Mobile, Inexpensive Device for Upper Extremity Rehabilitation at Home. In Proceedings of the IEEE 10th International Conference on Rehabilitation Robotics (ICORR). Noordwijk, The Netherlands, 13–15 June 2007; pp. 933–937.
13. Hesse, S.; Schulte-Tigges, G.; Konrad, M.; Bardeleben, A.; Werner, C. Robot-assisted arm trainer for the passive and active practice of bilateral forearm and wrist movements in hemiparetic subjects. *Arch. Phys. Med. Rehabil.* **2003**, *84*, 915–920. [CrossRef]

14. Palsbo, S.E.; Hood-Szivek, P. Effect of robotic-assisted three-dimensional repetitive motion to improve handmotor function and control in children with handwriting deficits: A nonrandomized phase 2 device trial. *Am. J. Occup.* **2012**, *66*, 682–690. [CrossRef] [PubMed]
15. Johnson, M.; Wisneski, K.; Anderson, J.; Nathan, D.; Smith, R. Development of ADLER: The activities of daily living exercise robot. In Proceedings of the 1st IEEE/RAS-EMBS International Conference on Biomedical Robotics and Biomechatronics, BioRobotics, Pisa, Italy, 20–22 February 2006; pp. 881–886.
16. Fluet, G.G.; Qiu, Q.; Saleh, S.; Ramirez, D.; Adamovich, S.; Kelly, D.; Parikh, H. Robot-assisted virtual rehabilitation (NJIT-RAVR) system for children with upper extremity hemiplegia. In Proceedings of the Virtual Rehabilitation International Conference. Haifa, Israel, 29 June–2 July 2009; pp. 189–192.
17. Rosati, G.; Zanotto, D.; Secoli, R.; Rossi, A. Design and control of two planar cable-driven robots for upper-limb neurorehabilitation. In Proceedings of the IEEE International Conference on Rehabilitation Robotics ICORR. Kyoto, Japan, 23–26 June 2009; pp. 560–565.
18. Kiguchi, K.; Esaki, R.; Tsuruta, T.; Watanabe, K.; Fukuda, T. An exoskeleton system for elbow joint motion rehabilitation. In Proceedings of the IEEE/ASME International Conference on Advanced IntelligentMechatronics (AIM). Volume 2, Port Island, Japan, 20–24 July 2003; pp. 1228–1233.
19. Rosen, J.; Brand, M.; Fuchs, M.B.; Arcan, M. A myosignal-based powered exoskeleton system. *Ieee Trans. Syst. Man Cybern. Part A Syst. Hum.* **2001**, *31*, 210–222. [CrossRef]
20. Durante, F.; Zobel, P.B.; Raparelli, T. Development of an active orthosis for inferior limb with light structure. Mechanisms and Machine Science. In Proceedings of the International Conference on Robotics in Alpe-Adria Danube Region, Torino, Italy, 21–22 June 2017; pp. 833–841. [CrossRef]
21. Ertas, I.H.; Hocaoglu, E.; Barkana, D.E.; Patoglu, V. Finger exoskeleton for treatment of tendon injuries. In Proceedings of the IEEE International Conference on Rehabilitation Robotics (ICORR). Kyoto, Japan, 23–26 June 2009; pp. 194–201.
22. Sacco, K.; Belforte, G.; Eula, G.; Raparelli, T.; Sirolli, S.; Geda, E.; Geminiani, G.C.; Virgilio, R.; Zettin, M.P.I.G.R.O. An active exoskeleton for robotic neurorehabilitation training driven by an electro-pneumatic control. *Mech. Mach. Sci.* **2018**, *49*, 845–853. [CrossRef]
23. Sarakoglou, I.; Tsagarakis, N.G.; Caldwell, D.G. Occupational and physical therapy using a hand exoskeleton based exerciser. In Proceedings of the IEEE/RSJ International Conference on Intelligent Robots and Systems (IROS), Sendai, Japan, 28 September–2 October 2004; pp. 2973–2978.
24. Pignolo, L.; Dolce, G.; Basta, G.; Lucca, L.F.; Serra, S.; Sannita, W.G. Upper limb rehabilitation after stroke: ARAMIS a "robo-mechatronic" innovative approach and prototype. In Proceedings of the 4th IEEE RAS & EMBS International Conference in Biomedical Robotics and Biomechatronics (BioRob), Rome, Italy, 24–27 June 2012; pp. 1410–1414.
25. Kawasaki, H.; Ito, S.; Ishigure, Y.; Nishimoto, Y.; Aoki, T.; Mouri, T.; Sakaeda, H.; Abe, M. Development of a Hand Motion Assist Robot for Rehabilitation Therapy by Patient Self-Motion Control. In Proceedings of the IEEE 10th International Conference on Rehabilitation Robotics (ICORR). Noordwijk, Netherlands, 13–15 June 2007; pp. 234–240.
26. Li, Q.; Wang, D.; Du, Z.; Song, Y.; Sun, L. sEMG Based Control for 5 DOF Upper Limb Rehabilitation Robot System. In Proceedings of the IEEE International Conference on Robotics and Biomimetics (ROBIO), Kunming, China, 17–20 December 2006; pp. 1305–1310.
27. Mayr, A.; Kofler, M.; Saltuari, L. ARMOR: An electromechanical robot for upper limb training following stroke. A prospective randomised controlled pilot study. *Handchir Mikrochir Plast Chir.* **2008**, *40*, 66–73. [CrossRef] [PubMed]
28. Gaponov, I.; Popov, D.; Lee, S.J.; Ryu, J.H. Auxilio: A portable cable-driven exosuit for upper extremity assistance. *International J. Control Autom. Syst.* **2017**, *15*, 73–84. [CrossRef]
29. Cheng, H.S.; Ju, M.S.; Lin, C.C.K. Improving elbow torque output of stroke patients with assistive torque controlled by EMG signals. *J. Biomech. Eng.* **2003**, *125*, 881–886. [CrossRef]
30. Vanderniepen, I.; Van Ham, R.; Van Damme, M.; Versluys, R.; Lefeber, D. Orthopaedic rehabilitation: A powered elbow orthosis using compliant actuation. In Proceedings of the IEEE International Conference on Rehabilitation Robotics (ICORR). Kyoto, Japan, 23–26 June 2009; pp. 172–177.
31. Song, R.; Tong, K.Y.; Hu, X.L.; Zheng, X.J. Myoelectrically Controlled Robotic System That Provide Voluntary Mechanical Help for Persons after Stroke. In Proceedings of the IEEE 10th International Conference on Rehabilitation Robotics (ICORR), Noordwijk, The Netherlands, 13–15 June 2007; pp. 246–249.
32. Turner, M.; Gomez, D.; Tremblay, M.; Cutkosky, M. Preliminary tests of an arm-grounded haptic feedback device in telemanipulation. In Proceedings of the the ASME Dynamic Systems and Control Division. Volume 64, Anaheim, CA, USA, 15-20 November 1998; pp. 145–149.
33. Mali, U.; Munih, M. HIFE-haptic interface for finger exercise. *Mechatron. Ieee/Asme Trans.* **2006**, *11*, 93–102. [CrossRef]
34. Hesse, S.; Kuhlmann, H.; Wilk, J.; Tomelleri, C.; Kirker, S.G.B. A new electromechanical trainer for sensorimotor rehabilitation of paralysed fingers: A case series in chronic and acute stroke patients. *J. Neuroeng. Rehabil.* **2008**, *5*, 21. [CrossRef]
35. Rotella, M.F.; Reuther, K.E.; Hofmann, C.L.; Hage, E.B.; BuSha, B.F. An Orthotic Hand-Assistive Exoskeleton for Actuated Pinch and Grasp. In Proceedings of the Bioengineering Conference, IEEE 35th Annual Northeast, Boston, MA, USA, 3–5 April 2009; pp. 1–2.

36. Wege, A.; Hommel, G. Development and control of a hand exoskeleton for rehabilitation of hand injuries. In Proceedings of the International Conference on Intelligent Robots and Systems (IROS 2005), Edmonton, Canada, 2–6 August 2005; pp. 3046–3051.
37. Burgar, C.G.; Lum, P.S.; Shor, P.C.; Van der Loos, H.F.M. Development of robots for rehabilitation therapy: The Palo Alto VA/Stanford experience. *J. Rehabil. Res. Dev.* **2000**, *37*, 663–673.
38. Amirabdollahian, F.; Loureiro, R.; Gradwell, E.; Collin, C.; Harwin, W.; Johnson, G. Multivariate analysis of the Fugl-Meyer outcome measures assessing the effectiveness of GENTLE/S robot-mediated stroke therapy. *J. Neuroeng. Rehabil.* **2007**, *4*, 4. [CrossRef]
39. Perry, J.C.; Rosen, J.; Burns, S. Upper-limb powered exoskeleton design. *Ieee/Asme Trans. Mechatron.* **2007**, *12*, 408–417. [CrossRef]
40. Mihelj, M.; Podobnik, J.; Munih, M. HEnRiE-Haptic environment for reaching and grasping exercise. In Proceedings of the 2nd IEEE RAS & EMBS International Conference on Biomedical Robotics and Biomechatronics (BioRob), Scottsdale, AZ, USA, 19–22 October 2008; pp. 907–912.
41. Sasaki, D.; Noritsugu, T.; Takaiwa, M. Development of Active Support Splint driven by Pneumatic Soft Actuator (ASSIST). In Proceedings of the IEEE International Conference on Robotics and Automation (ICRA), Barcelona, Spain, 18–22 April 2005; pp. 520–525.
42. Kline, T.; Kamper, D.; Schmit, B. Control system for pneumatically controlled glove to assist in grasp activities. In Proceedings of the 9th International Conference on Rehabilitation Robotics ICORR, Chicago, IL, USA, 28 June–1 July 2005; pp. 78–81.
43. Lucas, L.; Di Cicco, M.; Matsuoka, Y. An EMG-controlled hand exoskeleton for natural pinching. *J. Robot Mechatron.* **2004**, *16*, 482–488. [CrossRef]
44. Bouzit, M.; Burdea, G.; Popescu, G.; Boian, R. The Rutgers Master II-new design force-feedback glove. *IEEE/ASME Trans. Mechatron.* **2002**, *7*, 256–263. [CrossRef]
45. Klein, J.; Spencer, S.; Allington, J.; Bobrow, J.E.; Reinkensmeyer, D.J. Optimization of a parallel shouldermechanism to achieve a high-force, low-mass, robotic-arm exoskeleton. *Ieee Trans. Robot.* **2010**, *26*, 710–715. [CrossRef]
46. Takahashi, C.D.; Der-Yeghiaian, L.; Le, V.; Motiwala, R.R.; Cramer, S.C. Robot-based handmotor therapy after stroke. *Brain* **2008**, *131*, 425–437. [CrossRef]
47. Pylatiuk, C.; Kargov, A.; Gaiser, I.; Werner, T.; Schulz, S.; Bretthauer, G. Design of a flexible fluidic actuation system for a hybrid elbow orthosis. In Proceedings of the IEEE International Conference on Rehabilitation Robotics (ICORR), Kyoto, Japan, 23–26 June 2009; pp. 167–171.
48. Stienen, A.; Hekman, E.; Prange, G.; Jannink, M.; Aalsma, A.; van der Helm, F.; van der Kooij, H. Dampace: Design of an exoskeleton for force-coordination training in upper-extremity rehabilitation. *J. Med Devices* **2009**, *3*, 10. [CrossRef]
49. Stienen, A.H.A.; Hekman, E.E.G.; ter Braak, H.; Aalsma, A.M.M.; van der Helm, F.C.T.; van der Kooij, H. Design of a rotational hydro-elastic actuator for an active upper-extremity rehabilitation exoskeleton. In Proceedings of the 2nd IEEE RAS & EMBS International Conference on Biomedical Robotics and Biomechatronics (BioRob), Scottsdale, AZ, USA, 19–22 October 2008; pp. 881–888.
50. Umemura, A.; Saito, Y.; Fujisaki, K. A study on power-assisted rehabilitation robot arms operated by patient with upper limb disabilities. In Proceedings of the IEEE International Conference on Rehabilitation Robotics (ICORR), Kyoto, Japan, 23–26 June 2009; pp. 451–456.
51. Winter, S.H.; Bouzit, M. Use of Magnetorheological fluid in a force feedback glove. *Ieee Trans. Neural Syst. Rehabil. Eng.* **2007**, *15*, 2–8. [CrossRef]
52. Oda, K.; Isozumi, S.; Ohyama, Y.; Tamida, K.; Kikuchi, T.; Furusho, J. Development of isokinetic and iso-contractile exercisemachine MEM-MRB using MR brake. In Proceedings of the IEEE International Conference on Rehabilitation Robotics (ICORR), Kyoto, Japan, 23–26 June 2009; pp. 6–11.
53. Khanicheh, A.; Mintzopoulos, D.; Weinberg, B.; Tzika, A.A.; Mavroidis, C. MR_CHIROD v.2: Magnetic resonance compatible smart hand rehabilitation device for brain imaging. *Ieee Trans. Neural Syst. Rehabil. Eng.* **2008**, *16*, 91–98. [CrossRef]
54. Pedrocchi, A.; Ferrante, S.; Ambrosini, E.; Gandolla, M.; Casellato, C.; Schauer, T.; Klauer, C.; Pascual, J.; Vidaurre, C.; Gfoehler, M.; et al. MUNDUS project: MUltimodal Neuroprosthesis for daily upper limb support. *J. Neuroeng. Rehabil.* **2013**, *10*, 66. [CrossRef]
55. Nathan, D.E.; Johnson, M.J.; McGuire, J. Feasibility of integrating FES grasp assistance with a task-oriented robot-assisted therapy environment: A case study. In Proceedings of the 2nd IEEE RAS & EMBS International Conference on Biomedical Robotics and Biomechatronics (BioRob), Scottsdale, AZ, USA, 19–22 October 2008; pp. 807–812.
56. Kobayashi, H.; Nozaki, H. Development ofmuscle suit for supporting manual worker. In Proceedings of the IEEE/RSJ International Conference on Intelligent Robots and Systems (IROS), San Diego, CA, USA, 29 October–2 November 2007; pp. 1769–1774.
57. Xing, K.; Xu, Q.; He, J.; Wang, Y.; Liu, Z.; Huang, X. A wearable device for repetitive hand therapy. In Proceedings of the 2nd IEEE RAS & EMBS International Conference on Biomedical Robotics and Biomechatronics BioRob, Scottsdale, AZ, USA, 19–22 October 2008; pp. 919–923.
58. Raparelli, T.; Zobel, P.B.; Durante, F.; Antonelli, M.; Raimondi, P.; Costanzo, G. First clinical investigation on a pneumatic lumbar unloading orthosis. In Proceedings of the IEEE/ICME International Conference on Complex Medical Engineering, CME, Beijing, China, 23–27 May 2007; Volume 4381959, pp. 1327–1330. [CrossRef]

59. Gabrio Antonelli, M.; Beomonte Zobel, P.; Durante, F.; Raparelli, T. Development and pre-clinical investigation of a massage device for the low back. *Int. J. Mech. Eng. Technol.* **2018**, *9*, 742–754.
60. Koeneman, E.J.; Schultz, R.S.; Wolf, S.L.; Herring, D.E.; Koeneman, J.B. A pneumatic muscle hand therapy device. *Proc. Ieee Enginnering Med. Biol. Soc.* **2004**, *4*, 2711–2713. [CrossRef]
61. Balasubramanian, S.; Wei, R.; Perez, M.; Shepard, B.; Koeneman, E.; Koeneman, J.; He, J. RUPERT: An exoskeleton robot for assisting rehabilitation of arm functions. In Proceeding of International Conference on Virtual Rehabilitation, Vancouver, Canada, 25–27 August 2008; pp. 163–167.
62. Tsagarakis, N.; Caldwell, D. Development and control of a "soft-actuated" exoskeleton for use in physiotherapy and training. *J. Auton. Robot.* **2003**, *15*, 21–33. [CrossRef]
63. Durante, F.; Antonelli, M.G.; Beomonte Zobel, P. Development of an active exoskeleton for assisting back movements in lifting weights. *Int. J. Mech. Eng. Robot. Res.* **2018**, *7*, 353–360. [CrossRef]
64. Chou, C.-P.; Hannaford, B. Measurement and modeling of McKibben pneumatic artificial muscles. *Ieee Trans. Robot. Autom.* **1996**, *12*, 90–102. [CrossRef]
65. Antonelli, M.G.; Zobel, P.B.; D'Ambrogio, W.; Durante, F.; Raparelli, T. An analytical formula for designing McKibben pneumatic muscles. *Int. J. Mech. Eng. Technol.* **2018**, *9*, 320–337.
66. Sorge, F.; Cammalleri, M. A theoretical approach to pneumatic muscle mechanics. In Proceedings of the IEEE/ASME International Conference on Advanced Intelligent Mechatronics: Mechatronics for Human Wellbeing. AIM, Wollongong, NSW, Australia, 9–12 July 2013; Volume 6584228, pp. 1021–1026. [CrossRef]
67. Antonelli, M.G.; Beomonte Zobel, P.; Durante, F.; Raparelli, T. Numerical modelling and experimental validation of a McKibben pneumatic muscle actuator. *J. Intell. Mater. Syst. Struct.* **2017**, *28*, 2737–2748. [CrossRef]
68. Tondu, B.; Lopez, P. Modeling and Control of McKibben Artificial Muscle Robot Actuators. *Ieee Control Syst.* **2000**, *20*, 15–38. [CrossRef]
69. Antonelli, M.G.; Beomonte Zobel, P.; Durante, F.; Gaj, F. Development and testing of a grasper for NOTES powered by variable stiffness pneumatic actuation. *Int. J. Med Robot. Comput. Assist. Surg.* **2017**, *13*, e1796. [CrossRef]
70. Kiguchi, K.; Iwami, K.; Yasuda, M.; Watanabe, K.; Fukuda, T. An exoskeletal robot for human shoulder joint motion assist. *Ieee/Asme Trans. Mechatron.* **2003**, *8*, 125–135. [CrossRef]
71. Cozens, J.A. Robotic assistance of an active upper limb exercise in neurologically impaired patients. *Iiie Trans. Reha-Bilitation Eng.* **1999**, *7*, 254–256. [CrossRef]
72. Mavroidis, C.; Nikitczuk, J.; Weinberg, B.; Danaher, G.; Jensen, K.; Pelletier, P.; Prugnarola, J.; Stuart, R.; Arango, R.; Leahey, M.; et al. Smart portable rehabilitation devices. *J. Neuroenginnering Rehabil.* **2005**, *2*, 18. [CrossRef] [PubMed]
73. Stein, J.; Narendran, K.; McBean, J.; Krebs, K.; Hughes, R. Electromyography-controlled exoskeletal upper-limb-powered orthosis for exercise training after stroke. *Am. J. Phys. Med. Rehabil.* **2007**, *86*, 255–261. [CrossRef] [PubMed]
74. Kung, P.C.; Ju, M.S.; Lin, C.C.K. Design of a forearm rehabilitation robot. In Proceedings of the IEEE 10th International Conference on Rehabilitation Robotics ICORR, Noordwijk, The Netherlands, 12–15 June 2007; pp. 228–233.
75. Loureiro, R.C.V.; Belda-Lois, J.M.; Lima, E.R.; Pons, J.L.; Sanchez-Lacuesta, J.J.; Harwin, W.S. Upper limb tremor suppression in ADL via an orthosis incorporating a controllable double viscous beam actuator. In Proceedings of the 9th International Conference on Rehabilitation Robotics ICORR, Chicago, IL, USA, 28 June–1 July 2005; pp. 119–122.
76. Colombo, R.; Pisano, F.; Mazzone, A.; Delconte, C.; Micera, S.; Carrozza, M.C.; Dario, P.; Minuco, G. Design strategies to improve patientmotivation during robot-aided rehabilitation. *J. Neuroeng. Rehabil.* **2007**, *4*, 3. [CrossRef] [PubMed]
77. Dovat, L.; Lambercy, O.; Gassert, R.; Maeder, T.; Milner, T.; Leong, T.C.; Burdet, E. HandCARE: A cable-actuated rehabilitation system to train hand function after stroke. *Ieee Trans. Neural Syst. Rehabil. Eng.* **2008**, *16*, 582–591. [CrossRef]
78. Schabowsky, C.N.; Godfrey, S.B.; Holley, R.J.; Lum, P.S. Development and pilot testing of HEXORR. hand EXOskeleton rehabilitation robot. *J. Neuroeng. Rehabil.* **2010**, *7*, 36. [CrossRef]
79. Ho, N.S.K.; Tong, K.Y.; Hu, X.L.; Fung, K.L.; Wei, X.J.; Rong, W.; Susanto, E.A. An EMG-driven exoskeleton hand robotic training device on chronic stroke subjects: Task training system for stroke rehabilitation. Proceedings of IEEE International Conference on Rehabilitation Robot, Boston, MA, USA, 29 June–1 July 2011. [CrossRef]
80. Ögce, F.; Özyalçin, H. Case study: A myoelectrically controlled shoulder-elbow orthosis for unrecovered brachial plexus injury. *Prosthet. Orthosis Int.* **2000**, *24*, 252–255. [CrossRef]
81. Lum, P.; Reinkensmeyer, D.; Mahoney, R.; Rymer, W.Z.; Burgar, C. Robotic devices formovement therapy after stroke: Current status and challenges to clinical acceptance. *Top. Stroke Rehabil.* **2002**, *8*, 40–53. [CrossRef]
82. Gupta, A.; O'Malley, M.; Patoglu, V.; Burgar, C. Design, control and performance of RiceWrist: A force feedback wrist exoskeleton for rehabilitation and training. *Int. J. Robot. Res.* **2008**, *27*, 233. [CrossRef]
83. Gopura, R.A.R.; Kiguchi, K. A human forearm and wristmotion assist exoskeleton robot with EMG-based Fuzzy-neuro control. In Proceedings of the 2nd IEEE RAS & EMBS International Conference on Biomedical Robotics and Biomechatronics (BioRob), Scottsdale, AZ, USA, 19–22 October 2008; pp. 550–555.
84. Cordo, P.; Lutsep, H.; Cordo, L.; Wright, W.G.; Cacciatore, T.; Skoss, R. Assisted movement with enhanced sensation (AMES): Coupling motor and sensory to remediatemotor deficits in chronic stroke patients. *Neurorehabilit. Neural Repair* **2009**, *23*, 67–77. [CrossRef]

85. Kiguchi, K.; Kose, Y.; Hayashi, Y. Task-oriented perception-assist for an upper-limb powerassist exoskeleton robot. In Proceedings of the World Automation Congress (WAC), Kobe, Japan, 19–23 September 2010; pp. 1–6.
86. Gupta, A.; O'Malley, M. Design of a haptic arm exoskeleton for training and rehabilitation. *Ieee Asme Trans. Mechatron.* **2006**, *11*, 280. [CrossRef]
87. Lambercy, O.; Dovat, L.; Gassert, R.; Burdet, E.; Teo, C.L.; Milner, T. A haptic knob for rehabilitation of hand function. *Ieee Trans. Neural Syst. Rehabil. Eng.* **2007**, *15*, 356–366. [CrossRef] [PubMed]
88. Loureiro, R.C.V.; Harwin, W.S. Reach & Grasp Therapy: Design and Control of a 9-DOF Robotic Neuro-rehabilitation System. In Proceedings of the IEEE 10th International Conference on Rehabilitation Robotics (ICORR), Noordwijk, The Netherlands, 13–15 June 2007; pp. 757–763.
89. Koceska, N.; Koceski, S.; Durante, F.; Beomonte Zobel, P.; Raparelli, T. Control architecture of a 10 DOF lower limbs exoskeleton for gait rehabilitation. *Int. J. Adv. Robot. Syst.* **2013**, *10*, 68. [CrossRef]
90. Song, R.; yu Tong, K.; Hu, X. Assistive control system using continuous myoelectric signal in robot-aided arm training for patients after stroke. *Ieee Trans. Neural Syst. Rehabil. Eng.* **2008**, *16*, 371–379. [CrossRef] [PubMed]
91. Tong, K.Y.; Ho, S.K.; Pang, P.K.; Hu, X.L.; Tam, W.K.; Fung, K.L.; Wei, X.J.; Chen, P.N.; Chen, M. An Intention Driven Hand Functions Task Training Robotic System. In Proceedings of the Conference IEEE Engineering in Medicine and Biology Society, Buenos Aires, Argentina, 31 August–4 September 2010; Volume 2010, pp. 3406–3409.
92. Koceska, N.; Koceski, S.; Zobel, P.B.; Durante, F. Control architecture for a lower limbs rehabilitation robot system. In Proceedings of the 2008 IEEE International Conference on Robotics and Biomimetics, ROBIO, Bangkok, Thailand, 22–25 February 2009; Volume 4913131, pp. 971–976. [CrossRef]
93. Fleischer, C.; Kondak, K.; Wege, A.; Kossyk, I. Research on Exoskeletons at the TU Berlin. In Proceedings of the German Workshop on Robotics, Braunschweig, Germany, 9–10 June 2009.
94. Raparelli, T.; Beomonte Zobel, P.; Durante, F.; Raparelli, F. Development of a powered upper limb orthosis. In Proceedings of the 8th International Conference on Rehabilitation Robotics, ICORR, Taejon, Republic of Korea, 23-25 April 2003 (143-146).
95. Craig, J.J. *Introduction to Robotics: Mechanics and Control*, 3rd ed.; Pearson Education: London, UK, 2005.
96. Bourbonnais, F.; Bigras, P.; Bonev, I.A. Minimum-time trajectory planning and control of a pick-and-place five-bar parallel robot. *Ieee/Asme Trans. Mechatron.* **2014**, *20*, 740–749. [CrossRef]
97. Wang, D.; Wu, J.; Wang, L.; Liu, Y. A Postprocessing Strategy of a 3-DOF Parallel Tool Head Based on Velocity Control and Coarse Interpolation. *Ieee Trans. Ind. Electron.* **2018**, *65*, 6333–6342. [CrossRef]
98. Da Forno, R. *Dal Corpo Rigido al Robot con Matlab*; Mc Graw Hill Italia: Milano, Italy, 1998.
99. Pheasant, S. *Body Space: Anthropometry, Ergonomics and Design*; Taylor & Francis: London, UK, 1986.
100. Anatomylearning. Available online: https://anatomylearning.com/ (accessed on 29 August 2022).
101. Durante, F.; Raparelli, T.; Beomonte Zobel, P. Two-Dof Upper Limb Rehabilitation Robot Driven by Straight Fibers Pneumatic Muscles. *Bioengineering* **2022**, *9*, 377. [CrossRef]
102. Vlachos, E.; Jochum, E.; Demers, L.P. HEAT: The harmony exoskeleton self-assessment test. In Proceedings of the 2018 27th IEEE International Symposium on Robot and Human Interactive Communication (RO-MAN), Nanjing, China, 27–31 August 2018; pp. 577–582.
103. Bai, S.; Christensen, S.; Islam, M.R.U. An upper-body exoskeleton with a novel shoulder mechanism for assistive applications. In Proceedings of the 2017 IEEE International Conference on Advanced Intelligent Mechatronics (AIM), Munich, Germany, 3–7 July 2017; pp. 1041–1046.
104. Ebrahimi, A.; Groninger, D.; Singer, R.; Schneider, U. Control parameter optimization of the actively powered upper body exo-skeleton using subjective feedbacks. In Proceedings of the 3rd International Conference on Control, Automation and Robotics, ICCAR, Nagoya, Japan, 22–24 April 2017; pp. 432–437. [CrossRef]
105. Castro, M.N.; Rasmussen, J.; Andersen, M.S.; Bai, S. A compact 3-DOF shoulder mechanism constructed with scissors linkages for exoskeleton applications. *Mech. Mach. Theory* **2019**, *132*, 264–278. [CrossRef]
106. Strzelczyk, P.; Tomczewski, K.; Wrobel, K. The Middleware for an Exoskeleton Assisting Upper Limb Movement. *Sensors* **2022**, *22*, 2986. [CrossRef]